南京航空航天大学

论文集

（二〇〇〇年）

第16册

三院

南京航空航天大学科技部编

二〇〇一年六月

五　　院

○五三系

目 录

序号	姓名	职称	单位	论文题目	刊物、会议名称	年、卷、期	类别
486	朱剑英	教授	053	Agent-Based Intelligent Manufacturing System for the 21st Century	IMCC'2000(香港)	2000	
487	乔 兵 朱剑英	讲师	053	Fuzzy Modeling of Inverse Dynamics for Robot Manipulators Based on a Genetic Algorithm	Annals of the CIRP	004901	H
488	吴红芳 姜澄宇 王宁生	硕士	053	基于 CIMS 的车间控制器系统	机械设计与制造工程	002903	J
489	吴含前 姜澄宇 王宁生 田新成	博士	053	Pro/Intralink 在并行工程中的应用	机械设计与制造	000006	J
490	吴含前 姜澄宇 王宁生	博士	053	PDM 技术的发展	机械设计	001712	J
491	李 秀 姜澄宇 王宁生	博士	053	基于并行工程的产品开发过程建模	机械设计与制造工程	002901	J
492	李 秀 沈 晶 姜澄宇 王宁生	博士	053	Visual Basic 中控制输入输出口的方法	计算机工程与应用	003603	J
493	李 秀 姜澄宇 王宁生	博士	053	柔性生产线信息管理系统关键技术的实现	南京航空航天大学学报	003202	J
494	刘红星 姜澄宇 左洪福	博士后	053	基于矩阵奇异值分解的信号非周期性程度指标	南京航空航天大学学报	003201	J*
495	吉卫喜 王宁生	博士	053	基于 CIMS 的减速机成组生产与经营管理系统	中国机械工程	001104	H

一种三自由度并联机床位置正解的对偶空间方法

姚学升,姚 裕,李桥梁,吴洪涛
(南京航空航天大学 机电工程学院,江苏 南京 210016)

摘要:提出了一种实现三自由度平动的并联机床结构,并对其运动学进行了分析研究,提出一种对偶空间方法来获得封闭式位置正解,解决了所研究的三自由度平动并联机床的位置正解问题。

关键词:并联机床;位置正解;封闭解;对偶空间方法
中图分类号:TH113.2⁺2 **文献标识码**:A **文章编号**:1007-9483(2000)06-0003-02

Method of Dual Space Used for Position Kinematics about Parallel Machine Tools with 3 DOF

YAO Xue-sheng, YAO Yu, LI Qiao-liang, WU Hong-tao
(Nanjing University of Aeronautics and Astronautics, Jiangsu Nanjing, 210016, China)

Abstract: It describes the structure of parallel machine tool with three degrees of freedom. By its kinematics it presents a new method of dual space to solve the forward position kinematics and derive its closed-form.

Key words: Parallel Machine Tool; Position Kinematics; Closed-form Solution; Method of Dual Space

并联机构具有结构简单、刚度高、传动链短、精度高、成本低、负载能力强等优点,因而使其在工程中的应用具有很大的潜力。然而其简单的结构对应着复杂的运动学,特别是正向运动学求解尤其复杂,一些并联机构甚至无法求出封闭解,有时只得用迭代法求其数值解。迭代法有两个缺点:①迭代次数无法预知,计算所需的时间也无法预知,计算量过于庞大;②迭代法有时根本得不到正确的解。因此迭代法不能用于要求高速、实时性和高精度的工程中。目前求解并联机床正向运动学封闭解常用的方法是消元法,但消元过程过于复杂,产生高次多项式,会得到无用的增根。

1 新型 3-DOF 并联机构

本文从丰田型并联机床出发,通过设置其中的导轨和动平台的一些参数,提出了一种新型的三自由度并联机构。只需机构上保证同时驱动一对作动器,就可以实现动平台三自由度平动,无需增加附加的平动机构,可有效地减少杆件之间的干涉,故其适用范围颇广,其结构如图 1 所示。

图 1 中 $A_1A_2A_3A_4A_5A_6$ 为静平台,$B_1B_2B_3B_4B_5B_6$ 为动平台;$A_1C_1, A_2C_2, A_3C_3, A_4C_4, A_5C_5, A_6C_6$ 为导轨,两两沿对称轴 $\boldsymbol{n}_1, \boldsymbol{n}_2, \boldsymbol{n}_3$ 对称分布,对称轴 $\boldsymbol{n}_1, \boldsymbol{n}_2, \boldsymbol{n}_3$ 交于 O 点;其上相应的交点为 $B_1, B_2, B_3, B_4, B_5, B_6$ 和 $C_1, C_2, C_3, C_4, C_5, C_6$。如果分别从 B_1B_2、B_3B_4、B_5B_6 中点作 $\boldsymbol{n}_1, \boldsymbol{n}_2, \boldsymbol{n}_3$ 的平行线,交点为 O_1 点,定义 OO_1 点的距离就等于两平台中心间的距离。

当机床满足以下条件,就可以实现动平台的三自由度平动:导轨两两平行,即 $A_1C_1 // A_2C_2 // \boldsymbol{n}_1, A_3C_3 // A_4C_4 // \boldsymbol{n}_2, A_5C_5 // A_6C_6 // \boldsymbol{n}_3$;且满足 $A_1A_2 = A_3A_4 = A_5A_6 = B_1B_2 = B_3B_4 = B_5B_6$;同时,滑块 C_1 和 C_2,C_3 和 C_4,C_5 和 C_6,两两同步驱动。本文研究在这种配置条件下丰田型并联机床的位置正解问题。

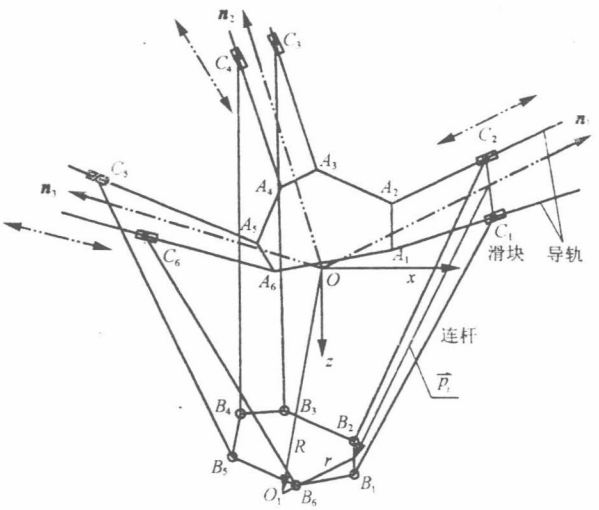

图 1 丰田型并联机床机构示意图

2 对偶空间方法求位置正解

2.1 运动方程的建立

如图 1 所示,将坐标系 xyz 设置在 O 点并使 $\boldsymbol{n}_1$ 在 zOx 平面内且与 x 轴的夹角为 β,则可以建立以下运动学方程:

$$L_0\boldsymbol{p}_1 - \boldsymbol{R} = (r-\xi)\boldsymbol{n}_i \overset{def}{=} \zeta\boldsymbol{n}_i \quad (i=1,2,3)$$
$$\zeta = (r-\xi) \tag{1}$$

收稿日期:2000-02-27;修订日期:2000-04-09
作者简介:姚学升(1973-),男,安徽无为人,南京航空航天大学在读硕士生,主要从事机床和机器人及其数控方面的研究。

式中，$\boldsymbol{R}$ 为动平台相对于静平台的位置矢量，ξ 为滑块的行程(成对驱动的两滑块中点到 O 点的距离)，r 为动平台两球铰点(与两平行连杆相连的点)中点到 O_1 点的距离，L_0 为连杆的长度，$\boldsymbol{p}_i$ 为连杆的单位方向矢量，满足 $\boldsymbol{p}_i \cdot \boldsymbol{p}_i = 1$。

由式(1)容易求位置反解：

$$L_0^2 = \boldsymbol{R}\cdot\boldsymbol{R} + 2(\boldsymbol{R}\cdot\boldsymbol{n}_i)(r-\xi_i) + (r-\xi_i)^2$$

解出：

$$\xi_i - r = \boldsymbol{R}\cdot\boldsymbol{n}_i \pm \sqrt{(\boldsymbol{R}\cdot\boldsymbol{n}_i)^2 + L_0^2 - (\boldsymbol{R}\cdot\boldsymbol{R})} \tag{2}$$

根据配置情况舍去负根。

2.2　正向运动学求解(位置正解)

正向运动学求解对于本结构就是已知滑块行程 ξ_i，求解动平台相对于静平台的位置矢量 $\boldsymbol{R}$，可将方程(1)改写成如下的矩阵形式：

$$\begin{bmatrix} L_0\boldsymbol{E} & 0 & 0 & -\boldsymbol{E} \\ 0 & L_0\boldsymbol{E} & 0 & -\boldsymbol{E} \\ 0 & 0 & L_0\boldsymbol{E} & -\boldsymbol{E} \end{bmatrix} \begin{bmatrix} \boldsymbol{p}_1 \\ \boldsymbol{p}_2 \\ \boldsymbol{p}_3 \\ \boldsymbol{R} \end{bmatrix} = \begin{bmatrix} \zeta_1\boldsymbol{n}_1 \\ \zeta_2\boldsymbol{n}_2 \\ \zeta_3\boldsymbol{n}_3 \end{bmatrix} \tag{3}$$

式中 $\boldsymbol{E}$ 为 3 阶单位矩阵。式(3)可简记为：

$$[A_{9\times12}]\{z\} = \{b\}$$

式中：$\{z\} \in R^{12}$ 张成了解域的 12 维空间 R^{12}，$\{b\} \in R^9$。

式(3)共有 12 个未知数，但只有 9 个线性方程组，这已知的 9 个线性方程组矩阵的行向量张成解空间 R^{12} 的一个子空间 V 的基矢量。现在取 A 的正交补矩阵 $A_\perp \in R^3$，满足 $A_\perp A^T = 0$，由观察可直接取自然正交补矩阵，$A_\perp = [-\boldsymbol{E}, -\boldsymbol{E}, -\boldsymbol{E}, \boldsymbol{L}_0\boldsymbol{E}]$，由 $A_\perp$ 可张成解域空间 R^{12} 的一个三维子空间，$V_\perp$ 称它为 V 的对偶空间。

于是得到以下线性方程组

$$\begin{bmatrix} A \\ A_\perp \end{bmatrix}\{z\} = \begin{bmatrix} b \\ \phi \end{bmatrix} \tag{4}$$

式中：$\{\phi\} \in R^{3\times1}$ 为一待定向量。可解出形式解

$$\{z\} = A^T(AA^T)^{-1}\{b\} + A_\perp(A_\perp A_\perp^T)^{-1}\{\phi\}$$

由 $\boldsymbol{p}_i \cdot \boldsymbol{p}_i = 1$　$(i = 1,2,3)$ 得非线性关系：

$$(\boldsymbol{p}_{i0}\cdot\boldsymbol{p}_{i0}) - \frac{1}{L_0^2+3}(\boldsymbol{p}_{i0}\cdot\boldsymbol{\phi}) + \frac{1}{(L_0^2+3)^2}(\boldsymbol{\phi}\cdot\boldsymbol{\phi}) = 1 \quad (i = 1,2,3) \tag{5}$$

式中：

$$\begin{cases} \boldsymbol{p}_{i0} = \dfrac{1}{L_0}\zeta_i\boldsymbol{n}_i - \dfrac{1}{L_0(L_0^2+3)}\sum\limits_{i=1}^{3}\zeta_i\boldsymbol{n}_i \\ \boldsymbol{R} = \dfrac{1}{L_0(L_0^2+3)}\sum\limits_{i=1}^{3}\zeta_i\boldsymbol{n}_i \end{cases}$$

将上式两两相减得到两个线性方程

$$\begin{cases} \boldsymbol{p}_{12}\cdot\boldsymbol{\phi} = \left(\dfrac{L_0^2+3}{2}\right)\xi_{12} \\ \boldsymbol{p}_{23}\cdot\boldsymbol{\phi} = \left(\dfrac{L_0^2+3}{2}\right)\xi_{23} \end{cases}$$

式中：

$$\begin{cases} \boldsymbol{p}_{12} = \boldsymbol{p}_{10} - \boldsymbol{p}_{20},\ \xi_{12} = \boldsymbol{p}_{10}\cdot\boldsymbol{p}_{10} - \boldsymbol{p}_{20}\cdot\boldsymbol{p}_{20} \\ \boldsymbol{p}_{23} = \boldsymbol{p}_{20} - \boldsymbol{p}_{30},\ \xi_{23} = \boldsymbol{p}_{20}\cdot\boldsymbol{p}_{20} - \boldsymbol{p}_{30}\cdot\boldsymbol{p}_{30} \end{cases} \tag{6}$$

补充正交方程：

$$(\boldsymbol{p}_{12}\times\boldsymbol{p}_{23})\cdot\boldsymbol{\phi} = \tau \quad (\tau \text{ 为一待定参数}) \tag{7}$$

联立方程式(6)，(7)得：

$$\boldsymbol{\phi} = [\boldsymbol{p}_{12},\boldsymbol{p}_{23}]\left[\begin{pmatrix}\boldsymbol{p}_{12}^T \\ \boldsymbol{p}_{23}^T\end{pmatrix}\cdot(\boldsymbol{p}_{12},\boldsymbol{p}_{23})\right]^{-1}\begin{pmatrix}\xi_{12} \\ \xi_{23}\end{pmatrix}\left(\frac{L_0^2+3}{2}\right) + (\boldsymbol{p}_{12}\times\boldsymbol{p}_{23})[(\boldsymbol{p}_{12}\times\boldsymbol{p}_{23})]^{-1}\tau \overset{def}{=} \boldsymbol{\phi}_1 + \boldsymbol{\phi}_2\tau$$

代入式(6)中的任一式，例如第一式，则可得关于 τ 的二次方程：

$$a\tau^2 + b\tau + c = 0 \tag{8}$$

式中：$a = \boldsymbol{\phi}_2\cdot\boldsymbol{\phi}_2$；$b = 2[\boldsymbol{\phi}_1\cdot\boldsymbol{\phi}_2 - (L_0^2+3)\boldsymbol{p}_{10}\cdot\boldsymbol{\phi}_2]$；

$c = \boldsymbol{\phi}_1\cdot\boldsymbol{\phi}_2 + (L_0^2+3)^2(\boldsymbol{p}_{10}\cdot\boldsymbol{p}_{10} - 1) - 2(L_0^2+3)\boldsymbol{p}_{10}\cdot\boldsymbol{\phi}_1$。

其解为：

$$\tau = \frac{-b \pm \sqrt{b^2 - 4ac}}{2a}$$

式中正、负号由导轨与静平台间的夹角决定，从而由 $\boldsymbol{\phi} = \boldsymbol{\phi}_1 + \boldsymbol{\phi}_2\tau$ 解出 $\boldsymbol{\phi}$，回代式(5)，$\boldsymbol{p}_i$ 和 $\boldsymbol{R}$ 即可得出。

2.3　位置正解算例

正向运动学求解的对偶空间方法较容易在计算机中实现，我们在 Matlab 环境下已设计了上述方法的应用程序。现举一例，取并联机床结构参数如下：$\beta = 18°$，$L_0 = 1$，$r = 0.3$。

假设 $\xi_1 = 1.081\ 5$，$\xi_2 = 0.977\ 5$，$\xi_3 = 1.435\ 1$，可据反解得出，由程序计算得到 τ 的两个解为 $\tau_1 = 0.754\ 4$，$\tau_2 = -0.042\ 8$；它们分别对应的位置矢量 $\boldsymbol{R}$ 为：$\boldsymbol{R}_1 = (-0.052\ 5, 0.193\ 2, -0.811\ 8)^T$，$\boldsymbol{R}_2 = (-0.070\ 7, 0.291\ 5, 0.254\ 3)^T$，将 $\boldsymbol{R}_1$，$\boldsymbol{R}_2$ 代入式(2)计算，与设定的 ξ_i 值完全一致，从而证实对偶空间方法正确有效。

3　结束语

本文提出的对偶空间方法实质上就是补充正交方程求解正向运动学。最终将位置正解问题转化为一元二次方程，得到了正确的封闭解，使位置正解问题得到了最简洁的描述，使用起来颇为方便。这种方法也适用于其它结构的并联机床，特别是作三自由度平动的并联机床，由于此类机床在工程实践上具有较大的应用潜力，因此本文所提出的位置正解方法对并联机床的研究、开发具有重要的指导意义。

参考文献：

[1]　李桥梁，吴洪涛 .3－DOF Stewart 机床结构设计[A]. 全国生产工程第 8 届学术年会暨第 3 届青年学者学术会议论文集[C]. 北京：机械工业出版社，1999.

[2]　黄　田，汪劲松 . 并联机床设计基础理论的研究进展[A]. 面向 21 世纪的中国振动工程研究[C]. 北京：航空工业出版社，1999.

[3]　吴　展，李桥梁，骆海峰，等 . 新型三自由度并联机床及其运动学模型的建立[J]. 淮海工学院学报，1999，8(4)：4－6.

文章编号:1004—132X(2000)06—0608—04

机械工程中的多体系统动力学问题

吴洪涛　熊有伦

吴洪涛　教授

摘要:介绍多体系统动力学在先进制造技术中的重要地位和作用。建议抓住机遇,迎接挑战,采取有力措施,推动我国多体系统动力学的应用与发展,使之有效地支撑我国的先进制造技术,提升我国机械和机电产品的国际竞争力。

关键词:先进制造技术;多体系统动力学;机械工程;机械工程应用

中图分类号:0313.7;TH16　　**文献标识码**:A

先进制造技术(AMT)以数控机床、加工中心、测量机、工业机器人等机电一体化设备组成先进制造系统,以网络和数据技术为特征,以CAD/CAM/CNC技术为基本支撑工具,其发展经历了柔性制造单元、柔性制造系统、集成控制系统、智能集成制造系统4个阶段。发达国家,前2个阶段技术已经成熟并实现了产业化,第三阶段处在开发完善阶段,智能化集成制造技术尚在研究探索中。有人将智能制造技术称为21世纪的先进制造技术。但无论如何,先进制造系统中的机电一体化设备是其实施的重要基础和关键。

1　多体系统动力学在先进制造技术中的作用与地位

机械工程学科在现代科学技术,特别是微电子技术、计算机技术迅猛发展的推动下,正在发展成为一门具有时代特征的学科,是20世纪后半叶"科学技术成为第一生产力"的具体表现。它导致了国民经济的支柱产业——机械工业正在发生而且还将继续发生极为深刻的变化,这一深刻的变化反映在,机械工程、机械工业的面貌和内容发生了根本性的变化,过去机械工程理论上主要以经典力学分析为基础,实践上主要以经验总结为基础,现在则体现为机械和电子的有机结合,其基础体现为,在深化和发展了的力学(即多体系统动力学)的基础上,与系统论、信息论、传感器理论、信号分析与处理、电子学、计算机、人工智能等多学科的交叉与融合。同时,它本身也正在形成自己的学科体系,即基于计算机应用的设计理论、工艺理论、先进制造技术理论等。机械产品的性质也正在发生重大的变化,机械产品与微电子学、微型计算机应用相结合,取代、延伸、加强与扩大了人脑的部分作用,机械制造技术正在彻底改造,从数控化走向柔性化、集成化、智能化,向先进制造技术发展,这已成为现代科学技术前沿的热点之一,也是国际高科技竞争的前沿。

机械工程的基础之一是一般力学,发展到今天,主要特征之一是多体系统动力学已经成为一般力学最活跃的领域,刘又午教授等认为,多体系统是对一般机械系统和机电系统的高度概括和总结。国际上基于多体系统动力学,已发展了ADAMS、DADS等十多种颇有影响的商业化软件,欧美的工程师应用此类软件生产复杂机械系统的"模拟样机",可真实地仿真运动过程,迅速地比较其多种参数的方案,直至获得优化的工作性能,从而大大地减少昂贵的物理样机制造及试验,提高产品设计质量和大幅度缩短产品研制周期,对市场作出快速响应。如同结构分析中的"有限元"理论,多体系统就是"机构"分析中的有限元,它可以将广大研究人员和技术人员从繁重的具体计算等事务性工作中解放出来,将精力集中到更高层次的目标上去。国内一些大学的力学系和少数机械系于十多年前开始跟踪国际前沿的研究,取得了许多重要的进展和成果,特别是在基础理论和方法上,但较之国外,我们在应用和软件的产业化方面还存在很大差距,而这恰好是我国当前所急需的。据统计,当前国际上可生产的各类产品有140多万种,然而我们目前仅能生产40多万种,为开发新产品所需的分析软件仍需要花费大量外汇进口,其差距由此可见一斑。因此,在当前制造业并行工程、敏捷制造、虚拟现实等先进制造技术哲理不断涌现和发展的条件下,产品设计、制造的"模拟样机"技术已经成为其中的极其关键的环节。正是基于这样的背景和认识,有理由认为我们应该加强对多体系统理论与应用进行孜孜不倦和系统深入的研究,使之成为我国先进制造技术的重要基础,从而促进其发展,进而推动我国的经济建设与持续发展。

收稿日期:2000—03—13

2　多体系统动力学的发展[1~5]

多体系统的动力学是综合了刚体力学、分析力学、计算力学、材料力学、生物力学等学科的成就，在航天、航空、机构学、机械制造、仿生假肢等机械工程领域经过多年应用实践逐步发展起来的一门古老而又高新的技术学科。北大西洋公约组织在1993年召开的高级技术研讨会把多体系统界定为刚性和柔性机械系统。实际上一般机械系统都是由若干物体以不同形式组合而成的，所以多体系统是一般机械系统的高度概括。一切复杂的刚体运动不外乎空间平动和定点转动的合成。18世纪50年代Euler提出了3个欧拉角，并导出了著名的运动学和动力学方程，奠定了点转动的理论基础。其后150年间人们只找到了3种特定情形下的第4个代数首次积分，即Euler(1758)、Lagrange(1788)、柯娃列夫斯卡娅(1888)的工作。本世纪初，Husson和Burgatti证明再无其它可积情形，不存在一般可积情形。此后研究方向转向工程技术的应用。

20世纪50年代以来科学技术和工业生产的发展，促使人们不得不面对多刚体系统。例如人造卫星的太阳帆板、航天飞机的机械臂、制造技术中的机器人、高速空间机构等。这类系统是刚体组合，但古典刚体力学无法解决这类系统的分析计算问题。首先是用什么数学工具描述多个物体之间的拓扑结构，以解决多体之间不同组合的多样性问题。其次是采用哪 种动力学方程以解算多个刚体以及多个动坐标耦合的问题。电子计算机的快速发展为解决上述问题提供了可能，但随之而来的是采用什么样的程序和软件体系以及合理的运动学和动力学参数才能完成快速高效准确计算。

进一步，从实践得知，实际上太阳帆板、航天飞机机械臂并非刚体。甚至某些高速精密机器人用多刚体模型描述也有较大误差。合理的方案当然是将这些构件考虑为柔性体。柔性体应用若干阶模态予以描述，模态的合理选择是关键。即使做必要的近似处理，也会使系统自由度大大增加。同时促使精确的动力学分析与近似的材料力学计算相互融合。随之而来的动力学方程复杂化和计算程序计算量扩大等问题有待研究解决。柔性体的大范围运动与高速小范围振动之间的刚柔耦合问题是又一个关键。在此情况下，动坐标架的选 取问题，动力学反解的多值性问题皆有待解决。鉴于应用领域的重要性和解决问题的艰巨性，使得多柔体系统动力学成为当前最具有挑战性的前沿课题。

由此可见，多体系统动力学问题是若干机械工程领域中的重要问题，同时也是一个具有挑战性的问题，具有重大的学术价值和工程实践意义。国外早在60年代，航天工程与机械工程领域的学者就已经各自独立地对多刚体系统动力学开展了研究，一般航天飞行器呈树状开环结构，在空间环境失重状态下运动；而机械系统通常是带闭环结构，作二维或三维运动。后来，此两领域的学者逐渐意识到其研究对象具有共同的理论基础，可应用统一的多体系统动力学加以研究。于是，一批力学家加入研究，例如Roberson、Wittenburg、Schielhen、Kane Huston等，促进了多体系统理论和方法的完善，同时又进一步推动了工程实际的应用，理论和实际相辅相成、相得益彰。当前国际上已经形成了若干多体系统理论的流派，如Roberson/Wittenburg方法、Kane/Huston方法、Newton/Euler方法、变分方法等，据此，发展了数十种分析软件，有的已经商业化。国内对于多体系统动力学的认识开始于1977年出版的Wittenberg著作的传入，以及Kane、Roberson、Wittenberg、Schiehlen、Huston等国际知名学者相继来访讲学，以及我国学者的出访。激起了我国力学、机械工程、航天工程等领域的科技工作者的广泛兴趣。十几年来，国内在理论研究和实际应用2个方面都取得了显著进步，形成了自己的特色。我们在一些单项技术和某些工程应用已经达到国际先进和领先水平，但总体上，还比较落后，特别是在具有自主版权的软件方面，还远远落后于国际，这种被动局面通过政策支持、学术界努力、工程界协作是完全可以改变的。同时，我们还应该清醒地认识到，在全球经济一体化、知识经济初见端倪的世纪之交，大力发展中华民族的软件产业，特别是多体系统动力学的软件产业，以期为我国的先进制造技术提供重要的技术支撑将是十分迫切的。随着我国航空、航天、机器人技术、机械工业等行业的发展，将对复杂的大型多体系统(包括机械、电子、液体晃动、控制等)提出越来越多、也更加复杂的分析要求，因此，国内多体系统动力学面临十分艰巨的任务。

3　抓住机遇，迎接挑战，推动我国多体系统动力学的应用与发展

多体系统动力学是一门新兴交叉学科，被认为是应用力学最活跃的领域之一，它植根与一般力学(动力学、振动、控制)的坚实基础之上，从机械工程、航天工程、车辆工程、仿生机械、机器人等应用领域中汲取营养，通过计算机应用发挥其强大的功能，因此成为机械工程大学科的前沿阵地，其进一

步发展对于我国的机械类学科建议，培养厚基础、宽口径、强能力的高素质人才具有极其重要的意义。另一方面，由于多体系统动力学的实践性，使之成为正在发展中的先进制造技术中科学先进而且卓有成效的分析设计方法，成为先进制造技术的若干重要支撑点之一。仅以多体系统理论在先进制造技术中应用为例，多体系统可以应用于各种机构、机床及机器人设计与研究，机床及机器人等先进制造技术中设备的误差研究与补偿，夹具设计、无夹具制造、形位误差评判等。实际上，误差评定和无夹具制造的理论是一致的，即通过调整实体模型的空间位姿使实际测量数据与理论模型吻合，当然它们以多体系统运动学理论为基础。此外多坐标数控机床的轨迹规划原理与串联机构的轨迹规划也是一致的，近年来发展迅速的并联机床(STEWART 机床)也是多体系统理论应用的一个重要领域，这是由于多体系统是对一般机械系统和机电系统的高度概括和总结这个特性所决定的。

综上所述，多体系统动力学理论与应用在我国的发展，将大大有助于新产品的技术开发，有助于提高国有企业技术水平，有助于我国机械产品走出“引进—消化—再引进”的怪圈，有助于缩小与发达国家的差距。

发展我国的多体系统动力学理论与应用，已经具有很好的基础，首先，党中央、国务院正在实施“科教兴国”的基本战略，提倡“科技创新与产业化”的指导思想，大力落实“科技是第一生产力”的正确方针，为科技创新及其产业化提供了良好的大气候。其次，我国的科技工作者通过艰苦努力、不断登攀，已经在多体系统动力学理论与应用方面积累了良好的基础，例如黄文虎、刘延柱、洪嘉振、陆佑方、陈滨、贾书惠、谢传锋、刘又午等学者领导的一批科研小组，在多体系统理论与应用方面取得了一系列的优秀成果，仅以刘又午教授及其助手们的工作为例，十多年来，对多体系统动力学的理论进行了系统、深入、卓有成效的研究，发展和完善了由著名力学家休斯敦教授提出的多体系统动力学的休斯敦方法。在多体系统动力学应用特别是在机械工程领域的应用方面取得了重要的进展，而且具备进一步扩大应用的前景[6~24]。

由此可见，当前，我们必须抓住机遇，迎接挑战，推动我国机械工程界对多体系统动力学的应用与发展，不仅十分迫切，也是十分有基础的。

参考文献：

[1] 熊有伦，吴波，丁汉. 新一代制造系统理论及建模. 中国机械工程，2000，11(1－2)：49～52

[2] 国家自然科学基金委员会. 优先领域战略研究报告——先进制造技术基础. 北京：高等教育出版社，1998.

[3] 熊有伦，罗欣，何汉武等. 先进制造技术——制造业走向 21 世纪. 世界科技研究与发展，1996，18(3－4)：31～40

[4] 熊有伦，张卫平. 制造科学——先进制造技术的源泉. 科学通报，1998，43(2)：337～344

[5] 休斯敦 R L，刘又午. 多体系统动力学(上册). 天津：天津大学出版社，1987：1～93

[6] 吴洪涛. 建立多刚体系统动力学方程的等价性. 天津大学学报，1993，26(3)：27～34

[7] WANG Shuxin，LIU Youwu，WU Hongtao. Dynamics of Multibody System Including Kinematics and Force Constraints. Chinese Journal of Mechanical Engineering(In English)，1993，6(4)：237～245

[8] ZHANG Dajun. Flexible Multibody System Dynamics：finite segment method. Chinese Journal of Mechanical Engineering (In English)，1994，(7)2：156～162

[9] ZHANG Dajun. The stiffness equation for finite segment method. Chinese Journal of Mechanical Engineering (In English)，1992，5(1)：23～30

[10] 刘又午. 计及动力刚化的柔性多体系统动力学分析. 天津大学学报，1998：31(4)：401～408

[11] 刘又午. 多体系统的脉冲响应. 机械工程学报，1991，27(3)：56～61

[12] 刘又午，吴洪涛. 采用辛算法提高多体系统动力学的计算精度. 天津大学学报，1994，27(6)：722～727

[13] 刘又午. 用实验模态分析确定工业机器人物理参数. 第四届机床设计研究会议论文集：北京：1987：89～94

[14] 王树新. 多臂机器人动力学. 天津大学学报(英文版). 1996，2(1)：7～11

[15] WU Hongtao，LIU Youwu，WANG Shuxin. Kinematics and Error Analysis for Multibody System. Chinese Journal of Mechanical Engineering (In English)，1994，7(1)：49～52

[16] 刘又午，吴洪涛. 多体系统理论在机构运动分析中的应用. 机械工程学报，1993，29(3)：104～112

[17] 王树新. 柔性机械臂的动力学分析与实验研究. 中国机械工程，1995，6(6)：18～20

[18] 刘才山. 柔性机械臂的动力学模型及滑模变结构控制. 振动与冲击，1998，17(1)：24～29

[19] ZHANG Qin. Geometric Error Identification for Numerical Control Machine Tool. Journal of Tianjin University，1995，1(2)：101～105

[20] ZHANG Qin. The methodology of Raising Location Accuracy for Numerical Control Machine Tool. Chinese Journal of Mechanical Engineering

New Hybrid Controller for Systems with Deterministic Uncertainties

Weiqing Huang and Lilong Cai, *Member, IEEE*

Abstract—**Improving both transient and steady-state response performances of systems is a challenging problem, especially in the face of system nonlinearities and uncertainties. In this paper, a new hybrid controller for systems with deterministic uncertainties is developed. The proposed controller identifies and compensates deterministic uncertainties simultaneously. It is the combination of a time-domain feedback controller and a frequency-domain iterative learning controller. The feedback controller decreases system variability and reduces the effect of random disturbances. The iterative learning controller shapes the system input to suppress the error caused by deterministic uncertainties such as friction and backlash. The control scheme use only local input and output information, no system model is required. The uncertainties can be structured or unstructured. The effectiveness of the proposed controller is experimentally verified on a servo system with gearbox.**

Index Terms—**Fourier series, learning control.**

I. Introduction

IN MODERN mechanical and electric systems, requirements on transient and steady-state response performances becomes more and more stringent. Zero-phase error tracking control (ZPETC) is a good solution for a linear time-invariant system with precise model. The control of systems that contain various uncertainties is an open research problem. Two major sources of uncertainties are friction and backlash. Friction is a nonlinear function of the velocity. Backlash is a common nonlinearity in mechanical transmission caused by unavoidable clearance between mechanical elements. Friction and backlash cause delays, oscillations, and inaccuracies in the position and velocity and consequently degrade the overall performance of the system. In the extreme case, they make the system unstable. Extensive research work has been done on friction compensation and the control of systems with unknown backlash. Based on an exact geometric backlash inverse model, Tao and Kokotovic proposed an adaptive control strategy with high gain. It requires that the actuator create an ideal impulse velocity to achieve an instantaneous move from one end of the backlash region to the other. In fact, impulse velocity is not realizable. The change of contact state will follow a transient response and settle at the desired position after a period of time. Tarng *et al.* proposed a method where a torque impulse, which decays exponentially, was fed into the driving mechanism to speed up the transient response. Yang and Fu considered the contact dynamic characteristics and proposed a "three mode" backlash model and a nonlinear adaptive controller. Ezal *et al.* used the model similar to that in [7] and reduced the harmful delay introduced by backlash by designing an optimal path for the backlash phase. Along the path the motor reaches the load fast and free of collision.

From the above research work we know that the effect of backlash cannot be completely eliminated without an anti-backlash device in the physical sense and the key point is to shorten the period of gear disengagement in the presence of system time-delay. Adding another input for compensation of friction and backlash is the most popular way. Two steps are involved in the friction and backlash compensation: friction and backlash identification and compensation input generation. Hence, adaptive learning control is a good solution.

The motivation of the learning control is utilizing the tracking error measured in the previous trial to improve the tracking performance in the present trial. Typically, it takes the form:

$$u_k(t) = u_{k-1}(t) + g\left(e_{k-1}(t)\right) \tag{1}$$

where k is the trial index; u_{k-1} and u_k are controller output in the previous and present trial respectively; $e_{k-1}(t)$ is the tracking error in the previous trial; and $g(\cdot)$ is a function of tracking error which determines various kinds of learning control algorithm. Arimoto *et al.* proposed a D-type learning control algorithm. Kawamura *et al.* introduced and analyzed P and PI type update law. Lee *et al.* applied the Fourier series to approximate the input–output characteristics and proposed a learning control algorithm for linear systems based on the approximation method. Huang *et al.* proposed a decentralized learning control scheme for robot manipulators. Gorinevsky *et al.* applied B-spline to approximate the input function and proposed a learning algorithm to obtain optimal feedforward by iteratively shaping the input function.

In this paper, we propose a new hybrid controller for the systems with deterministic uncertainties. It consists of a time-domain feedback controller and a frequency-domain iterative learning controller. The former reduces system variability and suppresses the effect of random disturbances and mismatch of initial condition. The later modifies the shape and phase of the system input suppressing the error caused by deterministic uncertainties such as backlash and friction. It forces each harmonic component of the error converges to zero in the frequency domain, so that the time-domain tracking error tends to zero. Hence, it enhances the stability and the performance of the closed-loop system. However, the methodology used here can only ensure to eliminate the error caused by deterministic

Manuscript received September 16, 1998; revised July 28, 1999. Recommended by Technical Editor T. J. Tarn. This work was supported by grants from the Hong Kong Research Grants Council.

W. Huang is with the Nanjing University of Aeronautics and Astronautics, Nanjing, China.

L. Cai is with the Department of Mechanical Engineering, The Hong Kong University of Science and Technology, Clear Water Bay, Hong Kong.

Publisher Item Identifier S 1083-4435(00)11062-2.

unknown dynamics since the learning control updated once a trial.

This paper is organized as follows. In Section II, the design of the hybrid controller is presented. The design of the learning controller in Fourier space is presented in Section III. The stability and convergence condition will be given in Section IV. The experimental results and discussions are present in Section V. Summary and conclusions are made in Section VI.

II. Design of a Hybrid Controller

Suppose a nonlinear deterministic system or plant P, such as geared servomotor, is controllable with output feedback only, and it has the following input–output relation

$$\tau(t) = f_P\left(\theta(t), t\right) \tag{2a}$$

and its response mapping is given by

$$\theta(t) = f_R\left(\tau(t), t\right) \tag{2b}$$

where $\tau(t)$ is input torque applied to system, $\theta(t)$ is the output and denotes the angular position. Given a desired trajectory $y^d(t)$ defined on the interval $[0, T]$, the iterative learning control problem is to find a learning algorithm defined by $f_L(\tau, \theta, \theta^d, t)$, such that the sequence of input produced by the iteration

$$\tau_k(t) = f_L\left(\tau_{k-1}(t), \theta_{k-1}(t), \theta^d(t), t\right) \tag{3}$$

converges to a fixed optimal function $\tau^*(t)$ and

$$\lim_{k\to\infty} \left\|\theta^d(t) - f_R\left(\tau^k(t), t\right)\right\| = \left\|\theta^d(t) - f_R\left(\tau^*(t), t\right)\right\| \tag{4}$$

is minimum on the interval $[0, T]$ in the sense of L_2 norm,

$$\|y(t)\| = \left(\frac{1}{T}\int_0^T y(t)^T y(t)\right)^{1/2}.$$

In general, the desired trajectory is continuous and lasts only finite duration. Therefore, it can be approximated by Fourier series with finite terms in the system's bandwidth. The magnitudes of every harmonic components of the desired trajectory are known constants. Similarly, the actual output of the system can also be approximated by Fourier series with the same format. Because the bases of the Fourier series are orthogonal in the given time duration, each harmonic components of the desired trajectory and/or the actual output are independent of each other. The tracking problem of making the output approach to the desired trajectory in time domain is equivalent to making each harmonic component of the actual output tend to that of the desired trajectory in frequency domain. The tracking problem in time domain is transformed to a number of independent regulation problems in Fourier space. We can therefore design a number of independent iterative learning controllers in Fourier space to make each Fourier coefficient of the actual output approach to corresponding Fourier coefficient of the desired trajectory. As a result, the tracking error in time domain will tend to zero. However, the response of the learning controller is slow. The controller parameters are updated once a trial. Hence, the controller output is updated once a trial. Within the trial duration, the control system is an open loop system. The learning control can only be applied to open loop stable systems or the systems have been stabilized. Also the learning controller would be easily disturbed by random disturbances and easily affected by mismatch of the initial condition. Therefore, a time-domain PD controller is applied deal with the random disturbance and decrease system variability while the learning controller is used to improve the tracking performance and the stability of the closed-loop system as well. The output of the PD controller is the input of the learning controller and indicates that the performance the controller has obtained, so the PD controller is a "sensor" of the learning controller. The iterative learning controller updates the output in very trial. The PD controller updates the output at every sampling period. The overall controller is the hybridization of a time-domain PD controller and a frequency-domain learning controller and is shown in Fig. 1.

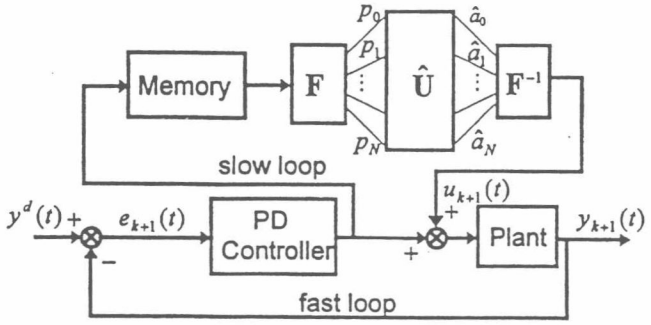

Fig. 1. The block diagram of the proposed controller.

III. Design of Learning Controller in Fourier Space

When we design the learning controller in Fourier space for a system, we assume that the system has the following properties.f

1) The internal dynamics of the system is stable, so that we may ignore its internal states and only use the output feedback instead of state feedback.
2) The desired trajectory of the system lasts for finite time duration T. Also, it complies with the actuator's capacity. In other words, the desired trajectory is physically reachable by the system.
3) The system has finite bandwidth. That is, the system can only respond to input of a certain frequency.

Subject to the above assumptions and according to theorems in Fourier analysis, the desired trajectory $\theta^d(t)$ of the system in the given time period of T can be approximated by a Fourier series with finite terms as follows.

$$\theta^d(t) = \frac{\mathrm{Re}\theta_0^d}{2} + \sum_{n=1}^{N}\left(\mathrm{Re}\theta_n^d \cos n\omega t + \mathrm{Im}\theta_n^d \sin n\omega t\right) \tag{5a}$$

$$\mathrm{Re}\theta_n^d = \frac{2}{T}\int_0^T \theta^d(t)\cos n\omega t dt, \qquad n = 0, 1, \ldots, N \tag{5b}$$

$$\mathrm{Im}\theta_n^d = \frac{2}{T}\int_0^T \theta^d(t)\sin n\omega t dt, \qquad n = 1, 2, \ldots, N \tag{5c}$$

where $\mathrm{Re}\,\theta_n^d$ and $\mathrm{Im}\,\theta_n^d$ are Fourier coefficients which are known constants, $\omega = 2\pi/T$ is the fundamental frequency.

The positive integer N is upper bounded and depends on the bandwidth of the system. In this way, the desired trajectory $\theta^d(t)$ is approximated by a summation of $(2N+1)$ harmonic sinusoidal and cosine functions with different constant magnitudes. In other words, $\theta^d(t)$ is transformed into Fourier space which takes $(2N+1)$ nonlinear functions as its coordinates or basis,

$$1, \cos\omega t, \cos 2\omega t, \ldots, \cos N\omega t, \sin\omega t, \sin 2\omega t, \ldots, \sin N\omega t \tag{6}$$

The elements of the basis are orthogonal in the time interval $[0, T]$. So the magnitudes (Fourier coefficients) are independent of each other. Similarly, in the kth trial, the actual output $\theta^k(t)$ of the system can also be approximated by Fourier series in the same time period $[0, T]$ as the following:

$$\theta^k(t) = \frac{\mathrm{Re}\theta_0^k}{2} + \sum_{n=1}^{N}(\mathrm{Re}\theta_n^k \cos n\omega t + \mathrm{Im}\theta_n^k \sin n\omega t) \tag{7a}$$

$$\mathrm{Re}\theta_n^k = \frac{2}{T}\int_{(k-1)T}^{kT} \theta^k(t)\cos n\omega t dt, \qquad n = 0, 1, \ldots, N \tag{7b}$$

$$\mathrm{Im}\theta_n^k = \frac{2}{T}\int_{(k-1)T}^{kT} \theta^k(t)\sin n\omega t dt, \qquad n = 1, 2, \ldots, N \tag{7c}$$

where k is the trial index. The upper bound of the harmonic terms N of $\theta^k(t)$ is the same as that of the desired trajectory. Because $\theta^d(t)$ is reachable by $\theta^k(t)$ according to assumption 2, and the frequency components of $\theta^k(t)$ is limited by the system bandwidth.

In the kth trial, the output angular error is defined as

$$\Delta\theta^k(t) = \theta^d(t) - \theta^k(t), \qquad k = 1, 2, \ldots \tag{8}$$

According to (8) and (9), the Fourier series of the tracking error in the kth trial $\Delta\theta^k(t)$is given by

$$\Delta\theta^k(t) = \frac{\mathrm{Re}E_0^k}{2} + \sum_{n=1}^{N}(\mathrm{Re}E_n^k \cos n\omega t + \mathrm{Im}E_n^k \sin n\omega t) \tag{9a}$$

$$\mathrm{Re}E_n^k = \mathrm{Re}\theta_n^d - \mathrm{Re}\theta_n^k, \qquad n = 0, 1, \ldots, N \tag{9b}$$

$$\mathrm{Im}E_n^k = \mathrm{Im}\theta_n^d - \mathrm{Im}\theta_n^k, \qquad n = 1, 2, \ldots, N. \tag{9c}$$

In each trial the desired trajectory $\theta^d(t)$ is the same, so that the Fourier coefficients of $\theta^d(t)$ are constants and are independent of the trial index k. Therefore, minimizing the norm $\|y^d(t) - y_k(t)\|$ in time domain is transformed into the problem of minimizing the norm of a $(2N+1)$ dimensional vector $[\mathrm{Re}\,\theta_n^d - \mathrm{Re}\,\theta_n^k,\ \mathrm{Im}\,\theta_n^d - \mathrm{Im}\,\theta_n^k]^T$ in Fourier space. Since the selected bases of Fourier space are orthogonal, all the Fourier coefficients in (9) are independent. We can design $(2N+1)$ independent controller to regulate each Fourier coefficient $\mathrm{Re}\,\theta_n^k$ and $\mathrm{Im}\,\theta_n^k$ individually. If each of the Fourier coefficients of $\theta^k(t)$ converges to that of $\theta^d(t)$ respectively, the Fourier coefficients of $\Delta\theta^k(t)$ will converge to zero. Hence, the output angular error in time domain will tend to zero.

The proposed controller is the combination of the learning controller and PD controller,

$$\tau^k(t) = \tau_{PD}^k(t) + \hat{\tau}^k(t). \tag{10}$$

where $\hat{\tau}^k(t)$ is the output of the learning controller which is the estimation of optimal input $\tau^*(t)$ and $\tau_{PD}^k(t)$ is the output of the PD controller in the kth trial. $\tau_{PD}^k(t)$ is given by

$$\tau_{PD}^k(t) = k_p\Delta\theta^k(t) + k_d\,\Delta\dot{\theta}^k(t). \tag{11}$$

where k_p and k_d are positive feedback gains, $\Delta\theta^k(t)$ and $\Delta\dot{\theta}^k(t)$ are angular position error and angular velocity error respectively which can be obtained by sensors. Applying the proposed controller to the system (2) we have the following relation

$$f_P\left(\theta^k(t),\, t\right) = \tau_{PD}^k(t) + \hat{\tau}^k(t). \tag{12}$$

Applying Fourier transform on both side of the above equation, we have

$$\begin{aligned}\frac{a_0^k}{2} + \sum_{n=1}^{N}\left(a_n^k \cos n\omega t + a_{N+n}^k \sin n\omega t\right) &= \frac{p_0^k + \hat{a}_0^k}{2} + \sum_{n=1}^{N}\left((p_n^k + \hat{a}_n^k)\cos n\omega t\right. \\ &\left. +(p_{N+n}^k + \hat{a}_{N+n}^k)\sin n\omega t\right). \end{aligned}\tag{13}$$

Here, a_n^k are Fourier coefficients of the system function $f_P(\theta^k(t), t)$, $\hat{a}_n^k$ are Fourier coefficients generated by the learning controller, and p_n^k are Fourier coefficients of τ_{PD}^k calculated by

$$p_n^k = \begin{cases} \dfrac{2}{T}\displaystyle\int_{(k-1)T}^{kT} \tau_{PD}^k(t)\cos n\omega t\, dt, & n = 0, 1, \ldots, N \\ \dfrac{2}{T}\displaystyle\int_{(k-1)T}^{kT} \tau_{PD}^k(t)\sin n\omega t\, dt, & n = N+1, \ldots, 2N. \end{cases} \tag{14}$$

Hence, the closed-loop system dynamic equations in Fourier space are obtained.

$$a_n^k = p_n^k + \hat{a}_n^k, \qquad n = 0, 1, \ldots, 2N;\ k = 1, 2, \ldots. \tag{15}$$

On the other hand, equation (11) indicates when $\tau_{PD}^k(t) = 0$ the tracking error $\Delta\theta(t)$ will approach zero and the best performance will be obtained. Hence, the controller design task is to develop an algorithm of $\hat{a}_n^k$, such that p_n^k tend to zero and $\hat{a}_n^k$ converges to its corresponding optimal value a_n^* as the trial number k increases. In other words, the learning algorithm should force $p_n^k + \hat{a}_n^k$ to approach constant a_n^*. Intuitively, we can design the update-law as

$$\hat{a}_n^k = \gamma_n \sum_{i=0}^{k-1} p_n^i \tag{16}$$

with $\gamma_n > 0$. The closed-loop system dynamic equation in Fourier space is

$$p_n^k + \gamma_n \sum_{i=0}^{k-1} p_n^i = a_n^k. \tag{17}$$

However, a_n^k is not a constant. It varies when p_n^k varies with the trial number k. For linear systems, the variation of p_n^k and a_n^k in one harmonic component is independent of other harmonics. For nonlinear systems, the variation in one harmonic component will alert other harmonic components, i.e. the harmonic components are cross-related. Hence, the condition $\gamma_n > 0$ is not sufficient to ensure p_n^k converge to zero. The sufficient condition for the system stability and convergence of the tracking error is discussed in the next section.

IV. Stability Condition of the Closed-Loop System

Defining $\Delta a_n^k = a_n^{k+1} - a_n^k$ and $\Delta p_n^k = p_n^{k+1} - p_n^k$. Δp_n^k denotes the variation of input from PD controller in the nth harmonic from the kth trial to the $(k+1)$th trial. Δa_n^k represents the change of system function due to the change of input. If the assumptions in Section III are satisfied, the sufficient condition for the system stability and convergence of the tracking error is given by the following theorem.

Theorem: When controller (10) with update-law (16) is applied to the system (2a) and (2b), the sufficient condition for the convergence of the tracking error is the learning gain $0 < \gamma_n < 1$ and the closed-loop system input–output relation in Fourier space satisfies $|(\Delta a_n^k / \Delta p_n^k)| < (1 - \gamma_n)$ for all n and k.

Proof: Applying the difference operator defined above to both sides of equation (15), we have

$$\Delta a_n^k = \Delta p_n^k + \Delta \hat{a}_n^k. \tag{18}$$

Applying the difference operator the update-law (16), we obtain

$$\Delta \hat{a}_n^k = \gamma_n p_n^k. \tag{19}$$

Substituting (19) into (18), we have the following relation

$$\Delta a_n^k = \Delta p_n^k + \gamma_n p_n^k \tag{20}$$

$$\frac{\gamma_n p_n^k}{\Delta p_n^k} = \frac{\Delta a_n^k}{\Delta p_n^k} - 1 \tag{21}$$

$$\gamma_n \Big/ \left(\frac{p_n^{k+1}}{p_n^k} - 1 \right) = \frac{\Delta a_n^k}{\Delta p_n^k} - 1 \tag{22}$$

$$\left| \frac{p_n^{k+1}}{p_n^{k1}} \right| = \left| \gamma_n \Big/ \left(\frac{\Delta a_n^k}{\Delta p_n^k} - 1 \right) + 1 \right|. \tag{23}$$

If the learning gain is selected from the range $0 < \gamma_n < 1$ and the closed-loop system satisfies $|(\Delta a_n^k / \Delta p_n^{k-1})| < (1 - \gamma_n)$, then we have

$$\left| \frac{p_n^{k+1}}{p_n^k} \right| \leq \beta < 1. \tag{24}$$

Thus, a sequence of Fourier coefficients of the PD controller output will be generated as the trial number k increases. It satisfies

$$|p_n^k| \leq \beta |p_n^{k-1}| \leq \beta^2 |p_n^{k-2}| \leq \ldots \leq \beta^k |p_n^0|. \tag{25}$$

Since the initial value p_n^0 is bounded, each Fourier coefficient of the PD controller output $\tau_{PD}^k(t)$ will diminish asymptotically as the trial number k increases. We will finally obtain the error equation in time domain,

$$k_P \, \Delta\theta(t) + k_D \, \Delta\dot{\theta}(t) = 0. \tag{26}$$

As k_P and k_D are positive constants, the above equation constructs a stable sliding surface. $\Delta\theta(t)$ will tend to zero along the sliding surface as time lasts, notice that $t = kT + t', t' \in (0, T)$, as $k \to \infty, t \to \infty$.

A. Remarks

1) Tracking errors come from two sources: the model uncertainties (structured and unstructured) and the random disturbances. The learning controller estimates the deterministic uncertainties from the historical input and output information, and reduces the tracking error by nearly perfect compensation for these uncertainties. The feedback controller reduces the effects of random disturbances and the mismatch of the initial condition. However, most of the present-day control methods attempt to suppress errors coming from different sources by one controller.
2) Both Δa_n^k and Δp_n^k vary with the trial number k. The condition $|(\Delta a_n^k / \Delta p_n^k)| < (1 - \gamma_n)$ gives a conservative robust bound. Its physical meaning is that the first derivative of a_n^k respect to p_n^k is less than 1 while the trajectory is carried out repeatedly. In linear systems, Δa_n^k and Δp_n^k are independent of other harmonic components, so that the actual bound of $|(\Delta a_n^k / \Delta p_n^k)|$ is smaller and the learning gain can be selected larger for fast convergence rate. In nonlinear systems, both Δa_n^k and Δp_n^k will be influenced by other harmonic components, the actual bound of $|(\Delta a_n^k / \Delta p_n^k)|$ will be larger. A smaller learning gain should be selected to ensure the stability. A larger learning gain corresponds to a faster convergence rate of the tracking error.
3) Although the proposed scheme is a linear method in Fourier space when constant learning gains are used, the generated Fourier series can represent the nonlinear optimal input function and the nonlinear input–output relation in time domain. Hence, it can be applied to nonlinear systems to compensate nonlinear uncertainties. Since the controller only uses measurable input and output information, there is no requirement for the state equation model. This approach is particularly useful when not all state variables are measurable.
4) The number of harmonic terms should be selected based on the bandwidth of the closed-loop system and the frequency components of the desired trajectory. The number of harmonic terms is limited by resonant frequency of the

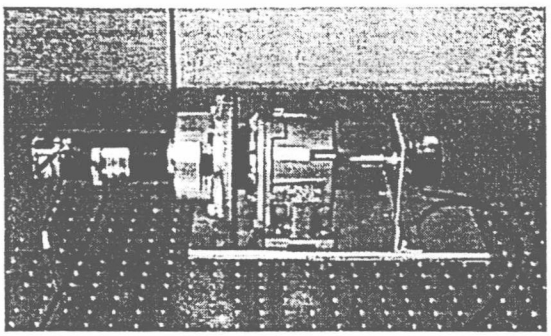

Fig. 2. Setup of dcservo motor driven gearbox.

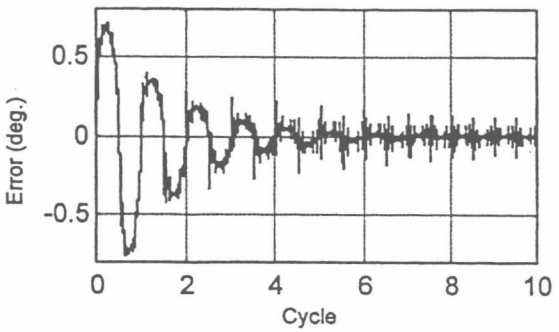

Fig. 3. Tracking error of the system with $k_p = 0.04$, $k_d = 0.0002$, $\gamma = 0.5$, $N = 20$.

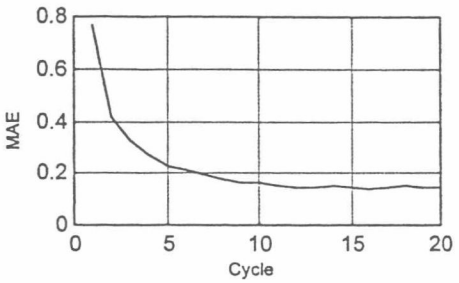

Fig. 4. Maximum absolute of the error with $k_p = 0.04$, $k_d = 0.0002$, $\gamma = 0.5$, $N = 20$.

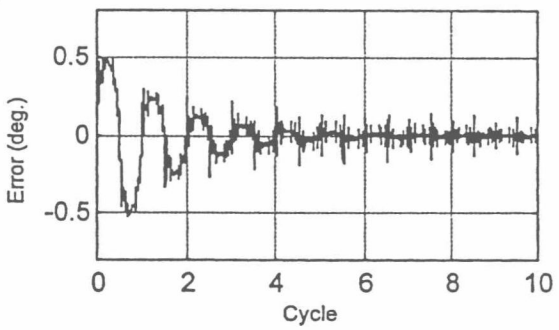

Fig. 5. Tracking error of the system with $k_p = 0.06$, $k_d = 0.00025$, $\gamma = 0.5$, $N = 20$.

system, which could not be included in the learning controller. The larger the harmonic terms are, the more harmonic components of the output error will be canceled and well performance will be obtained.

V. Experimental Results and Discussion

Illustrative experiments have been conducted on a dc motor driven commercial gearbox (Fig. 2). The gearbox has a double-reduction gear train. The reduction between input shaft and output shaft is 9.31 : 1. An optical rotary encoder with a resolution of 5000 lines/rev is mounted on the output shaft. A PC486-60 equipped with an A/D, D/A card and a decoder card is applied to carry out the control algorithm. The program is written in C language. The sampling frequency is 1 kHz.

In our experiments, the angular position of the output shaft used for feedback was measured by the optical rotary encoder and the velocity was obtained by numerically differentiating the position signal with respect to time. The desired output angular position trajectory is given by

$$\theta^d(t) = 45^\circ(1 - \cos 2\pi t)(\text{deg.})t \in [0, 1).$$

Its velocity crosses zero, so friction and backlash effect the tracking performance. The desired trajectory lasts only one second. Therefore, tracking the desired trajectory one second is considered as a trial. In the experiments, we used the same learning control gain for each component in Fourier space, i.e., $\gamma_0 = \gamma_1 = \gamma_2 = \cdots = \gamma_{2N} = \gamma$.

The experimental results of the angular position tracking error is shown in Fig. 3. Here, we can see clearly the convergent procedure of the tracking error. Since the learning gain is less than 1 ($\gamma = 0.5$), the tracking error converges to a small band after eight trials. The position error cannot converge to zero even after 20 trials. This is because of the existence of random disturbances. The effect of friction and backlash is reduced; however, small tracking error peaks still exist at the moment when the motor changes the rotary direction due to physical limitation on the compensation of backlash. In the learning controller the harmonic terms of the Fourier series is $N = 20$, that is, only those frequency components lower than 19 Hz are covered. To eliminate the spark which has very rich frequency components, N must be large enough to cover all frequency components of the spark. However, the increase of N is limited since the resonant frequency of the controlled system cannot be included. Also, required computation will increase with the increase of N.

For a convenient comparison of the system performance, we use two performance indices: the integral of the square of the error (ISE) and the maximum absolute of the error (MAE).

$$\text{ISE} = \int_{kT}^{(k+1)T} e^2(t)\,dt \qquad k = 0, 1, 2, \ldots$$
$$\text{MAE} = \max(|e(t)|) \qquad kT < t < (k+1)T$$

MAE is the index to measure the compensation of static friction and backlash, as shown in Fig. 4; the effects of static friction and backlash are reduced as trial number increases.

A. Contributions of the PD Controller

We have tested the proposed control scheme with different PD gains. Fig. 5 shows the tracking error of the system with $k_p = 0.06$ and $k_d = 0.00025$. Comparison of ISE index is

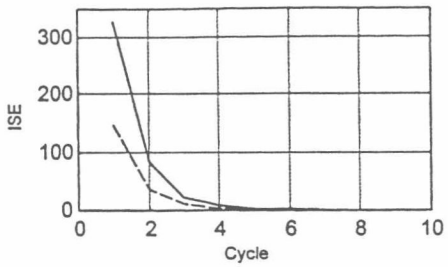

Fig. 6. ISE index. $k_p = 0.04$, $k_d = 0.0002$ (solid line), $k_p = 0.06$, $k_d = 0.00025$ (dash line), $\gamma = 0.5$, $N = 20$.

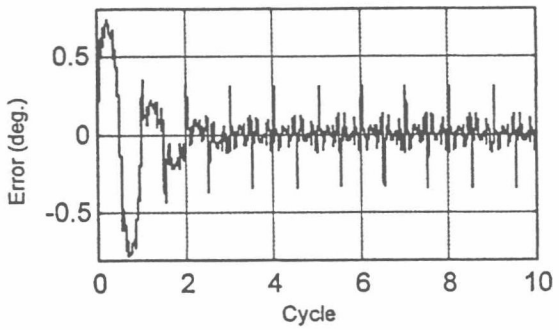

Fig. 7. Tracking error of the system with $k_p = 0.04$, $k_d = 0.0002$, $\gamma = 0.5$, $N = 10$.

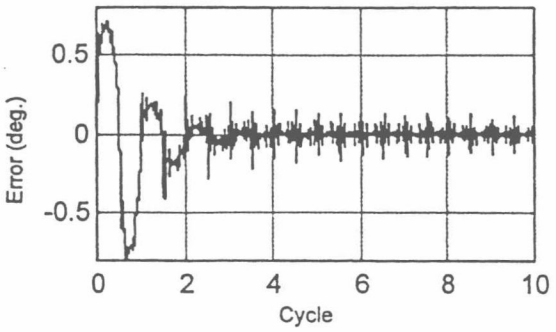

Fig. 8. Tracking error of the system with $k_p = 0.04$, $k_d = 0.0002$, $\gamma = 0.75$, $N = 20$.

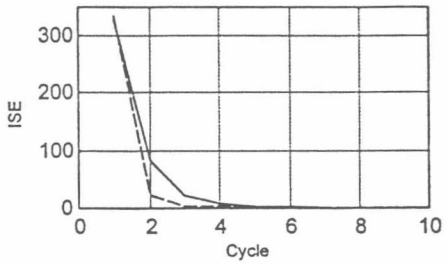

Fig. 9. ISE index with $k_p = 0.04$, $k_d = 0.0002$, $N = 20$, $\gamma = 0.5$ (solid line) and $\gamma = 0.75$ (dash line).

shown in Fig. 6. Although PD gains did not influence the convergent rate, it does yields a smaller initial error. The PD gains also have a minor influence on the final value of the error, since the system is disturbed by random noise. The performance with higher PD gains is a little better than that with smaller gains because increasing PD gains will reduce the effect of random disturbances. The PD controller also constructs a sliding surface, so the gains k_p and k_d should be tuned according to the characteristics of the system and disturbances.

B. Effectiveness of the Harmonic Terms

Fig. 7 shows the experimental result with reduced harmonic term number. By comparing Figs. 3 and 7, we can see that the convergent rates are nearly the same. However, after the tracking error converges, higher error peaks are left in Fig. 7. This is because that error spark contains higher frequency components. To compensate that, the input signal should also have higher frequency components. The number of harmonic terms should be as larger as possible considering of the control performance, the computational speed and the resonant frequency of the system.

C. Effectiveness of the Learning Gains

Fig. 8 shows the experimental results with a larger learning gain ($\gamma = 0.75$). Fig. 9 shows the comparison of the performance index with different learning gains. From Fig. 9, we can see that larger learning gain is corresponding to fast convergent rate. Learning gain should be selected according to the system's nonlinearity with consideration of system stability. For a highly nonlinear system, γ should be smaller to ensure that the system is asymptotically stable.

D. Effectiveness of Phase Compensation

To investigate the mechanism of the proposed control scheme to reduce the tracking error, we compare the controller output before and after learning. The controller output $u_1(t)$ in the first trial (only use PD control) and $u_8(t)$ in the eighth trial (after learning) are shown in Fig. 10. From which, we know that $u_1(t)$ and $u_8(t)$ have half-wave symmetry. Therefore, when we choose cosine format Fourier series $[f(t) \approx a_0 + \sum_{n=1}^{N} A_n \cos(n\omega t + \theta_n)]$ for $u_1(t)$ and $u_8(t)$, the terms for odd values of n are dominant terms (i.e., $|A_n|$ is larger). Their amplitudes and phases are shown in Table I. It is clear from this table that there is not much difference in amplitudes, the distinguished difference between $u_1(t)$ and $u_8(t)$ is in their phases. Each dominant harmonic component of $u_8(t)$ has a leading phase to $u_1(t)$. These leading phases give $u_8(t)$, in time domain, a leading time to $u_1(t)$, which can been seen from Fig. 10. Such phase leading compensates the system time-delay which varies with the input frequency. Therefore, we understand that phase compensation is very important for the improvement of the control performance. We also find from the table that each harmonic component of $u_8(t)$ has similar phase.

The lead phase for the compensation of time-delay varies with input frequency and is difficult to obtain. Therefore, compensation of time-delay cannot be simply completed by inducing a constant lead time in feedforward. Also, this problem is difficult to solve by designing a linear or nonlinear controller in time domain. The proposed controller learns both magnitude and phase information from the history of the system input and output and automatically achieves the best compensation of system time-delay.

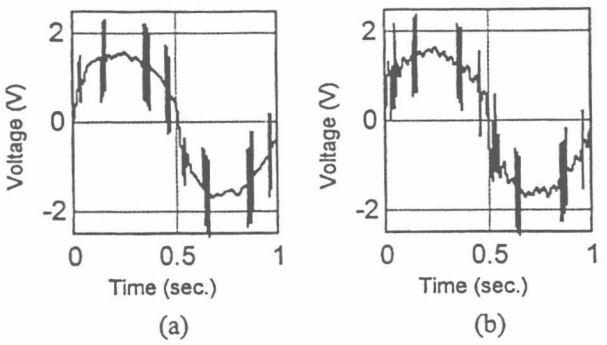

Fig. 10. (a) Output voltage $u_1(t)$. (b) Output voltage $u_8(t)$.

TABLE I
AMPLITUDES AND PHASES OF THE CONTROLLER OUTPUT VOLTAGES

Fre.	Amplitude		Phase (degree)	
(Hz)	$u_1(t)$	$u_8(t)$	$u_1(t)$	$u_8(t)$
1	1.767	1.77	-88.30	-86.88
3	0.274	0.250	-103.84	-93.97
5	0.129	0.114	-114.29	-90.99
7	0.090	0.087	-117.68	-84.47
9	0.059	0.061	-131.08	-81.88
11	0.053	0.054	-139.27	-79.93
13	0.045	0.049	-152.00	-73.90
15	0.045	0.056	-182.90	-86.59
17	0.026	0.051	-205.73	-83.09
19	0.036	0.062	-250.43	-90.05

VI. CONCLUSIONS

In this paper, a new hybrid control scheme is presented. Both theoretical analysis and experimental results have shown that the proposed control scheme is effective and has some special features compared with many others. In the design of the proposed controller, we neither use the model of the plant nor use models of friction and backlash. It is a model-free method. The learning controller is designed in Fourier space with orthogonal bases. The desired trajectory, system input, actual output and tracking error are represented by independent harmonic components. Therefore, the nonlinear tracking control problem in time domain is simplified to a number of independent regulation problems in frequency domain. Since the phase information of each component is included in the pairs of Fourier coefficients, the controller can obtain the system input with optimal magnitudes and optimal phases. With the phase information, the controller can compensate the system time-delay effectively. Besides the learning controller, a PD controller is also applied so that the effects of random disturbances and mismatch of initial condition is much reduced. The robustness of the learning controller is improved. Also, the control scheme is easy for implementation.

ACKNOWLEDGMENT

The authors would like to thank the reviewers and the editors for their constructive comments and suggestions.

REFERENCES

[1] S. Arimoto, S. Kawamura, and F. Miyazaki, "Bettering operation of robots by learning," *J. Robot Syst.*, vol. 1, no. 2, pp. 123–140, 1984.
[2] C. Canudas de Wit, P. Noel, A. Aubin, and B. Brogliato, "Adaptive friction compensation in robot manipulators: Low velocities," *Int.J. Robot. Res.*, vol. 10, no. 3, pp. 189–199, 1991.
[3] K. Ezal, P. V. Kokotovic, and G. Tao, "Optimal control of tracking systems with backlash and flexibility," in *Proc. 36th IEEE Conf. on Decision and Control*, 1997, pp. 1749–1754.
[4] J. W. Filbert and G. C. Winston, "Adaptive compensation for an optical tracking telescope," *Automatica*, vol. 10, pp. 125–131, 1974.
[5] D. Gorinevsky, D. E. Torfs, and A. A. Goldenberg, "Learning approximation of feedforward control dependence on the task parameters with application to direct-drive manipulator tracking," *IEEE Transactions on Robotics and Automat.*, vol. 13, no. 4, pp. 567–580, 1997.
[6] W. Huang, L. Cai, and X. Tang, "Decentralized learning control for robot manipulators," in *Proc. 1999 IEEE Int. Conf. on Robotics & Automation*, 1999, pp. 843–848.
[7] T. Kavli, "Frequency domain synthesis of trajectory learning controllers for robot manipulators," *J. Robot. Syst.*, vol. 9, pp. 663–680, 1992.
[8] S. Kawamura, F. Miyazaki, and S. Arimoto, "Realization of robot motion based on a learning method," *IEEE Trans. Syst., Man, Cybern.*, vol. 18, pp. 126–134, 1988.
[9] H. S. Lee and M. Tomizuka, "Robust motion controller design for high-accuracy positioning systems," *IEEE Trans. Ind. Electron.*, vol. 43, pp. 48–54, 1996.
[10] J.-W. Lee, H.-S. Lee, and Z. Bien, "Iterative learning control with feedback using Fourier series with application to robot trajectory tracking," *Robotica*, vol. 11, pp. 291–298, 1993.
[11] K. L. Moore, *Iterative Learning Control for Deterministic Systems*. New York: Springer-Verlag, 1993.
[12] N. Sadegh and K. Gugliemo, "A new repetitive controller for mechanical manipulators," *J. Robot. Syst.*, vol. 8, no. 4, pp. 507–529, 1991.
[13] G. Tao and P. V. Kokotovic, "Adaptive control of systems with unknown output backlash," *IEEE Trans. Automat. Contr.*, vol. 40, pp. 326–330, 1995.
[14] Y. S. Tarng, J. Y. Kao, and Y. S. Lin, "Identification of and compensation for backlash on the contouring accuracy of CNC machining centers," *Int. J. Adv. Manufact. Technol.*, vol. 13, no. 2, pp. 77–85, 1997.
[15] M. Tomizuka, "Zero phase error tracking algorithm for digital control," *Journal of Dynamic Systems, Measurement, and Control*, vol. 109, no. 3, pp. 65–68, 1987.
[16] M. Vidyasagar, *Nonlinear Systems Analysis*. Englewood Cliffs, NJ: Prentice Hall, 1993.
[17] J.-H. Yang and L.-C. Fu, "Nonlinear adaptive control for manipulator system with gear backlash," in *Proc. 35th IEEE Conf. on Decision and Control*, 1996, pp. 4369–4374.

Weiqing Huang received the B.E. and M.Phil. degree in mechanical engineering from Nanjing University of Aeronautics and Astronautics, China, in 1987 and 1990 respectively, and the Ph.D. degree in mechanical engineering from the Hong Kong University of Science and Technology in 1999.

From 1990 to 1995, he worked as an Engineer in Nanjing University of Aeronautics and Astronautics, Nanjing, China. Currently, he is a Lecture in the Department of Mechanical Engineering, Nanjing University of Aeronautics and Astronautics.

Lilong Cai received the Ph.D. degree in mechanical engineering from the University of Toronto, Canada, in 1990.

He is an Assistant Professor in the Department of Mechanical Engineering, the Hong Kong University of Science and Technology. From 1990 to 1993, he was an Assistant Professor in the Department of Mechanical Engineering, Columbia University, New York City. He has published more than 20 referred journal papers and over 40 international conference papers in the area of robotics, nonlinear control application, mechatronics and precision measurement using laser technology. He is also the co-inventor of two U.S. patents.

第 32 卷第 1 期　　南京航空航天大学学报　　Vol. 32 No. 1
2000 年 2 月　　Journal of Nanjing University of Aeronautics & Astronautics　　Feb. 2000

基于 Internet 的远程 FMS 故障诊断系统研究

陈　希　　楼佩煌
（南京航空航天大学 CIMS 工程研究中心　南京，210016）

摘要　柔性制造系统(Flexible manufacturing system，FMS)是综合了机械、电子、管理、自动控制、计算机等先进技术的机电一体化制造系统。它组成的设备多、控制复杂，因而系统故障处理的难度高，能否实现快速的故障诊断和处理将影响 FMS 的推广和应用。文中运用 Internet 中基于 Web 的数据库技术探讨了如何对 FMS 故障进行异地、多专家协同诊断的可行性，提出了基于 Internet 的远程 FMS 故障诊断系统的基本结构和功能。

关键词：柔性制造系统；故障诊断；数据库；因特网
中图分类号：TH165；TP306；TP311.13

引　言

柔性制造系统(Flexible manufacturing system，FMS)是一组数控加工、清洗及检测设备通过自动化物料储运系统(包括物料流和刀具流)连接起来的用以制造一族零件的制造系统，并在计算机网络和数据库系统等支撑技术的支持下，实现制造过程的自动化。它综合了机械、电子、管理、自动控制、计算机等许多先进技术。由于系统中各种机械、电子元器件繁多，相互联系，相互依赖，这就使得系统故障率大，处理的难度也较大。尽管在系统的设计和开发过程中采用科学合理的方法，在使用过程中进行定期维护和保养都可以大大降低 FMS 的故障率。但对于这样复杂的系统，保证不出故障几乎是不可能的，一旦出现故障，能否对故障进行快速的诊断，并排除故障，对于一个 FMS 来说是非常重要的。

目前，故障检测与诊断系统的主要形式有[1]：(1)离线故障检测与诊断；(2)单机在线故障检测与诊断；(3)集中式在线故障检测与诊断。离线工况检测与故障诊断通过检测传感器采集设备运行信息，由计算机分析、诊断。这种方式经济方便，但一般只适用于定期检测。单机在线故障检测与诊断方式对每一个工作单元安装一套故障检测诊断系统。这种方式实时性好，可靠性高，各检测与诊断子系统的信息不能共享。集中式在线故障检测与诊断方式克

收稿日期：1999-03-31；修改稿收到日期：1999-05-26
第一作者：陈　希，男，硕士生，1976 年 10 月生。